

Influence of the Electrical Field on the Vibrating Signal Conversion in Electrochemical (MET) Motion Sensor

Vadim Agafonov, Egor Egorov

Moscow Institute of Physics and Technology, Institutsky Lane 9, Dolgoprudny, Moscow Region, 141700

*E-mail: agvadim@yandex.ru, egorovev@mail.ru

Received: 14 November 2015 / *Accepted:* 5 December 2015 / *Published:* 1 February 2016

The subject of the studies presented in the paper is four-electrode electrochemical cell used as a signal conversion element in molecular-electronic transfer (MET) motion sensors. Two outer electrodes of the cell (anodes) are maintained at higher potential relative to two internal ones (cathodes) and variations of the cathodic currents due to the mechanical motion of the electrolyte solution are considered the cell output signal. In case the cell is manufactured by microelectronic methods, the distance between the electrodes could be very small ($\leq 10\mu\text{m}$) and the cathodic electrical current becomes sensitive to the agents concentration on anodes. This effect was not taken into account in earlier considered cells with a larger distance between the electrodes. In the paper, the theoretical model which takes into account the influence of the electrical potential distribution in the solution on the active agents concentration on anodes and correspondingly on the cathodic current has been proposed. Analytical analysis of the model displays earlier unknown and practically important effect of the conversion factor growth for configurations with a large distance between the cathodes compared to the distance between a cathode and the adjacent anode.

Keywords: Electrochemical cell, MET sensor, convective diffusion, potassium iodide, iodide, tri-iodide, hydrodynamics.

1. INTRODUCTION

Symmetrical four-electrodes electrochemical cell is used as a sensing element in MET (molecular-electronic transfer), or electrochemical, motion sensors [1, 2]. In this application, the electrodes are placed inside a channel filled with electrolyte solution. Usually the electrical potential of 0.3-0.8 V is applied between the electrodes, so that two external electrodes serve as anodes, while the internal ones serve as cathodes. This configuration is known as ACCA (anode-cathode-cathode-anode)

[2]. Technologically, the practical cell is made of gauze electrodes separated by porous dielectric spacers. The distance between the electrodes is in the range 50-200 μm . The solution is water based highly concentrated iodide salt with a small amount of tri-iodide. The operation principle exploits the fact that the electrical current in saturation regime is very sensitive to liquid motion. So, if an external mechanical signal generates motion of the liquid, it changes the current passing through the electrodes. The difference between the cathodic currents is considered MET transducer output current.

Practical advantage of the MET sensor is the ability to provide a high conversion factor with a very simple and suitable for mass production [3] signal converting system. The MET sensors are used in seismology [5, 6, 7, 8], navigation [7] and structural monitoring [8].

The primary method for theoretical analysis of the cell response to mechanical motion uses the convection-diffusion equation for tri-iodide ions transfer. Other ions are not taken into consideration. Such approach implies the fact that tri-iodide ions participate in all reactions on the electrode surface and associated electron flow determines the electrical current completely. The advantage of this approach is the simplicity of mathematical formulation, which allows to lean on analytical methods and to decrease the requirements for computer resources in numerical simulation.

Meanwhile, the approach based on the convection-diffusion equation meets both theoretical and experimental difficulties. From the theoretical point of view, it is difficult to formulate the boundary conditions on the anodes [11, 12]. Frequently used conditions of constant concentration or constant electrical current density across the anodes surface fail to describe the anodic current changes with the increase of the mechanical signal frequency. In reality, as it is shown in [9], the concentration and density of the anodic current do not remain constant. In the meantime, for practically used cells with specific inter-electrode distance of about 100 μm , the influence of anodic concentrations changes on the differential cathodic current is little and the mentioned difficulty still allows getting quite exact results for the cell output current in the convection-diffusion equation.

Recently, a number of researchers have reported on the successful implementation of the microelectronic technologies to produce a four-electrode electrochemical cell [2, 13]. In this design, the distance between the electrodes is significantly decreased to the level of ~ 1 μm or even less. At that, the influence of the anodic concentration changes on the output cathodic currents cannot be neglected. This difficulty inspires the researches to use more complicated and resource-demanding methods [2, 3, 14, 15] based on Nernst-Plank equations and Butler-Volmer type boundary conditions.

In this paper, we aimed to find the signal converting cell response by combining the convection-diffusion equation with a more accurate formulation of the boundary conditions. The theoretical model starts with Nernst-Plank equations and with the boundary conditions that take into account the kinetics of the reaction on the electrodes. Assuming the smallness of active component concentration relative to the background electrolyte concentration, both the equations and the boundary conditions were significantly simplified. The resulting mathematical model includes the convection-diffusion equation for the active component concentration and Laplace type equation for electrical potential. On the electrodes, the boundary conditions bound tri-iodide concentration and the electrical potential. So, the influence of the electrical field is taken into account via modification of the boundary conditions.

In the paper [15], the same approach was successfully applied to find the relations between anodic and cathodic currents in a simple one-dimensional model of four-electrode electrochemical cell, with the geometrical parameters of the signal converting cell typical for gauze type cells. The results appeared critically different from the usual convection-diffusion model and correlated with the experimental data. Here, the same model for the most practical in the MET technology problem, which is modelling of the cathodic currents difference, was applied. Unlike previous studies, the cells with very short distance between the electrodes were taken into consideration. Based on the modelling, a new method to increase the signal converting factor in a wide frequency range has been found.

2. THEORY

Figure 1 illustrates the basic concept of MET sensing element, consisting of four electrodes configured as anode-cathode-cathode-anode (ACCA), separated by dielectric spacers, span the channels filled with electrolyte containing iodide ions. Holes through the electrodes and dielectric spacers allow the fluid to flow through the channels. The solution is $KI + I_2$ water-based electrolyte. According to the practical situation, KI is present in much higher concentration than I_2 . Potassium iodide dissolves into positive K^+ and negative I^- ions. Iodine I_2 is present in the form of tri-iodide ions I_3^- .

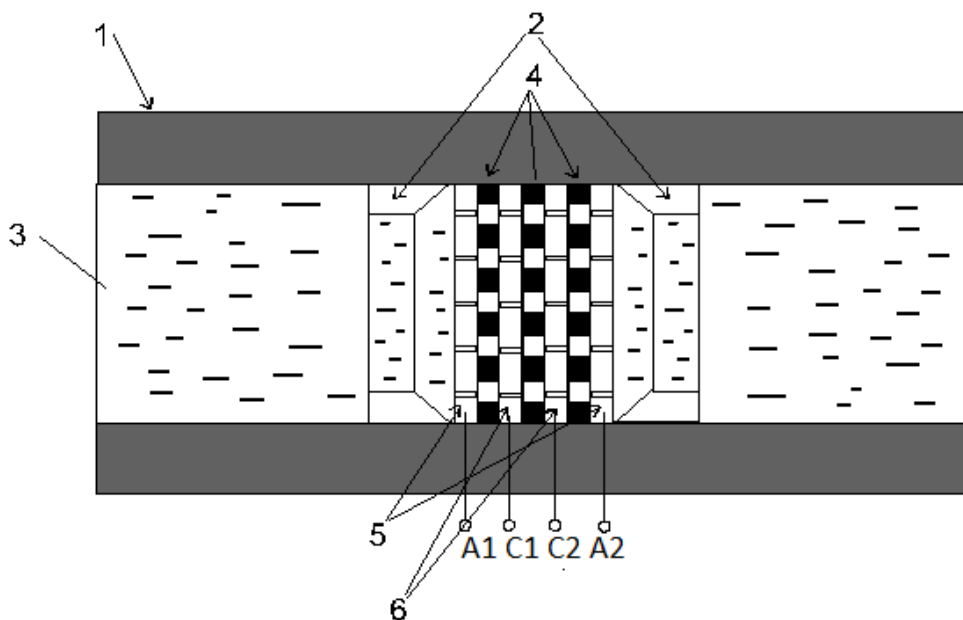


Figure 1. Basic concept of the electrochemical (MET) cell.

Legend:

- 1 – channel walls;
- 2 – members to fix electrodes in the channel;
- 3 – electrolyte;
- 4 – porous dielectric spacers ;
- 5 – external electrodes (anodes);
- 6- internal electrodes (cathodes).

Consider a mathematical model of the charge transfer in the solution volume. Start the analysis with the continuity equation:

$$\partial C_n / \partial t + \text{div } \vec{j}_n = 0 \tag{1}$$

C_n, \vec{j}_n are the concentration and the flow density for the n-th kind of ions. $n = I_3^-, I^-, K^+$. Flow densities are presented by the sum of diffusion $\vec{j}_{n,D}$, migration $\vec{j}_{n,m}$ and convection $\vec{j}_{n,c}$:

$$\begin{aligned} \vec{j}_n &= \vec{j}_{n,D} + \vec{j}_{n,m} + \vec{j}_{n,c} \\ \vec{j}_{n,D} &= -D_n \nabla C_n \\ \vec{j}_{n,m} &= -z_n D_n q C_n \nabla \phi / kT \\ \vec{j}_{n,c} &= \bar{V} C_n \end{aligned} \tag{2}$$

Herein ϕ is the electrical potential, q is the positive charge, which is equal to the absolute value of the electron charge, D_n is the diffusion coefficient of the n-th kind of ions, \bar{V} is the local hydrodynamic velocity, which should be determined from the equations of hydrodynamics. $z_{K^+} = 1, z_{I^-} = z_{I_3^-} = -1$.

The equations (2) are complemented by the condition of electroneutrality:

$$C_{K^+} - C_{I^-} - C_{I_3^-} = 0 \tag{3}$$

The usual conditions $C_{I_3^-} \ll C_{I^-}, C_{I_3^-} \ll C_{K^+}$ allow to simplify the problem. Let's follow [12, 17] and introduce a small parameter $\varepsilon \sim C_{I_3^-} / C_b \sim \delta C_{I^-} / C_b \sim \delta C_{K^+} / C_b$, where $\delta C_{I^-} = C_{I^-} - C_b$, $\delta C_{K^+} = C_{K^+} - C_b$. C_b denotes the K^+ concentration in the electrolyte bulk in equilibrium. Considering $\varepsilon \ll 1$, the migration term could be neglected in the equation for I_3^- transfer and $\vec{j}_{I^-,m} = \mu_{I^-} q C_b \nabla \phi$, $\vec{j}_{K^+,m} = \mu_{K^+} q C_b \nabla \phi$. So, keeping in **Error! Reference source not found.** and **Error! Reference source not found.** only the main terms, results in the following set of equations:

$$\begin{cases} \partial C_{I_3^-} / \partial t - D_{I_3^-} \Delta C_{I_3^-} + \bar{V} \nabla C_{I_3^-} \\ \partial C_{I^-} / \partial t - D_{I^-} \Delta C_{I^-} + \mu_{I^-} q C_b \Delta \phi + \bar{V} \nabla C_{I^-} = 0 \\ \partial C_{K^+} / \partial t - D_{K^+} \Delta C_{K^+} - \mu_{K^+} q C_b \Delta \phi + \bar{V} \nabla C_{K^+} = 0 \end{cases} \tag{4}$$

Calculating the sum of the first and the second equations, subtracting the third equation and applying the electroneutrality condition give Laplace type equation for potential

$$\Phi = \phi - \frac{kT(D_{I^-} - D_{K^+})C_{I^-}}{qC_b(D_{I^-} + D_{K^+})} - \frac{kT(D_{I_3^-} - D_{K^+})C_{I_3^-}}{qC_b(D_{I^-} + D_{K^+})}$$

(4) results in the following:

$$\begin{cases} \frac{\partial C_{I_3^-}}{\partial t} = D_{I_3^-} \Delta C_{I_3^-} - \bar{V} \nabla C_{I_3^-} \\ \Delta \Phi = 0 \end{cases} \tag{5}$$

Note that according to equation (2), the electrical current density is given by the following:

$$\vec{j}_e = q(\vec{j}_{K^+,s} - \vec{j}_{I_3^-,s} - \vec{j}_{I^-,s}) = -\sigma \nabla \Phi \tag{6}$$

Here $\sigma = \frac{q^2 C_b (D_{I^-} + D_{K^+})}{kT}$.

In formulating the boundary conditions, firstly take into account that there are no electrochemical reactions on dielectric surfaces:

$$\vec{j}_e = \vec{j}_{I_3^-,s} = 0 \tag{7}$$

At the electrode-electrolyte interface, the charge transfer is associated with the following electrochemical reaction:



The forward reaction takes place on anodes and the opposite one on cathodes. Therefore, the electrical current is linked to I_3^- flow:

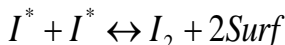
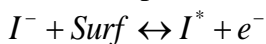
$$\vec{j}_{e,s} = 2q\vec{j}_{I_3^-,s} \tag{9}$$

The current passing through the electrode could be found by integrating the electrical current density over the electrode surface:

$$J_{el} = - \oint_{Sel} (\vec{n}, \vec{j}_{e,s}) dS \tag{10}$$

\vec{n} is the outer normal to the electrode surface. The current J_{el} is considered positive if the positive charge is transferred from the electrolyte to the electrode.

Use assumption [10] that the reaction (8) has three subsequent stages:



I^* denotes the adsorbed molecular iodine, *Surf* denotes the free surface of the electrode.

The interfacial electrical current density i_{el} is associated with the first stage of the mechanism (11) and, assuming that the major part of the electrode surface is free of adsorbed iodide, so rate of the forward reaction does not depend on the electrode surface coverage by adsorbed iodine, is given by:

$$i_{el} \equiv -(\vec{n}, \vec{j}_{e,s}) = q\vec{k}C_{I^*}^s - q\vec{k}C_{I^-}^s \tag{12}$$

$C_{I^*}^s$ is the concentration of the adsorbed iodine I^* and $C_{I^-}^s$ is the I^- concentration near the electrode surface, \vec{k} and \vec{k} denote the rate constants for the forward and reverse reactions.

Taking into account the dependence of the activation energy on the potential and Arrhenius equation, the expression for the current density could be modified as follows:

$$i_{el} = q\vec{k}_0 C_{I^*0}^s \left[\frac{C_{I^*}^s}{C_{I^*0}^s} e^{-\frac{\alpha q E}{kT}} - \frac{C_{I^-}^s}{C_{I^-0}^s} e^{-\frac{(1-\alpha)qE - qE_0}{kT}} \right] \tag{13}$$

$E = \varphi_{metal} - \varphi_{electrolyte}$ is the electrical potential drop across the double layer on the electrode surface, α is the electron transfer coefficient. Index 0 marks the values corresponding to equilibrium.

The second and the third stages in (11) are fast. So, the reagents are in equilibrium with reaction constants $K_2 = \frac{C^s_{I_2}}{C^s_{I^*2}}$ and $K_3 = \frac{C^s_{I_3^-}}{C^s_{I^-} C^s_{I_2}}$. Using the $\varepsilon \ll 1$ condition, we should assume

that $\frac{C^s_{I^-}}{C^s_{I^-0}} \approx 1$ and (13) results into the following:

$$i_{el} = q\vec{k}_0 C^s_{I^*0} \left[e^{\frac{(1-\alpha)qE - q\varepsilon_0}{kT}} - \sqrt{\frac{C^s_{I_3^-}}{C^s_{I_3^-0}}} e^{\frac{-\alpha qE}{kT}} \right] \tag{14}$$

In case of the of fast electrochemical reactions $\vec{k}_0 \rightarrow \infty$, and (13) could be transformed into:

$$\frac{C^s_{I_3^-}}{C^s_{I_3^-0}} = e^{\frac{2qE - q\varepsilon_0}{kT}} \tag{15}$$

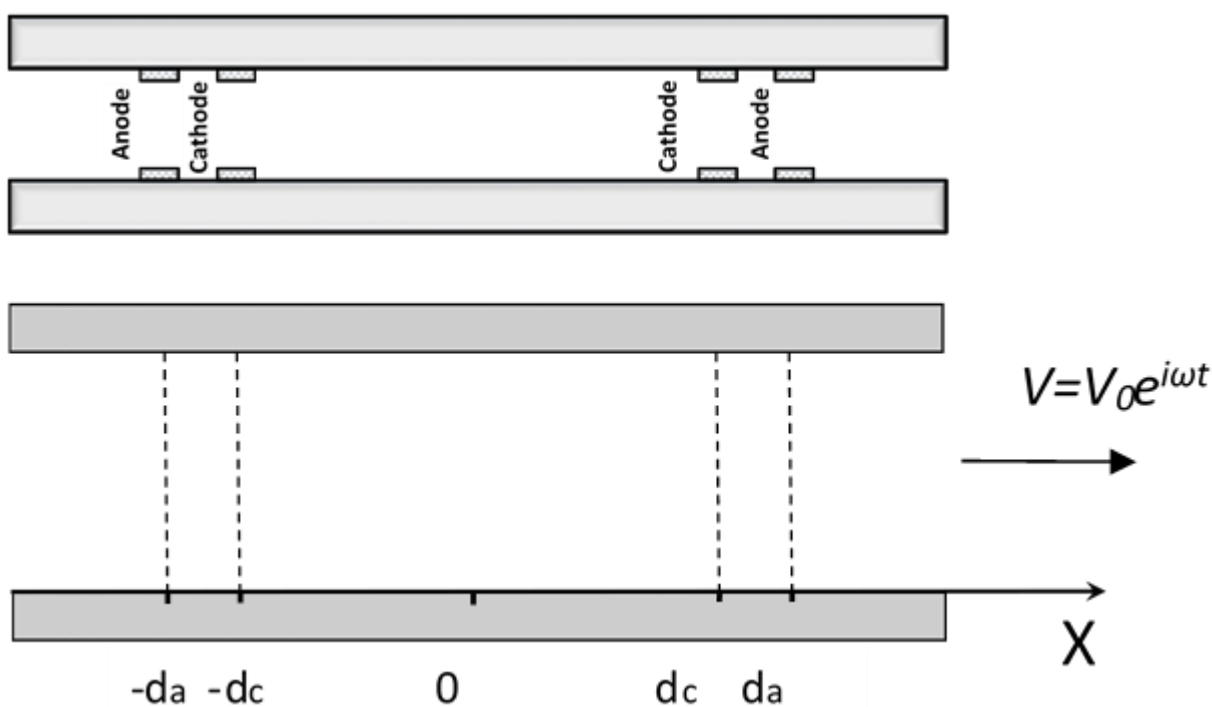


Figure 2. The one-dimensional MET signal converting cell model (lower part of the Figure) and its correspondence to planar cell (the upper part). Planes located at $\pm d_c$ and $\pm d_a$ denote the cathodes and anodes, correspondingly.

Finally, considering $\varepsilon \ll 1$, replace $\varphi_{electrolyte}$ with modified potential Φ on the electrode surface, so $E = \varphi_{metal} - \Phi$, and get the following condition:

$$\frac{C_{I_3^-}^s}{C_{I_3^-0}^s} = e^{\frac{2q(\varphi_{metal}-\Phi)-q\varepsilon_0}{kT}} \tag{16}$$

Equations (5) with the boundary conditions (7) for dielectric surfaces and (9), (15) for the electrodes give the mathematical formulation of charge transfer problem general for different configurations. Here, similar to [15] let's find a solution in the simplest one-dimensional model of a signal converting cell, schematically shown in Figure 2. The symmetrically placed infinite planes penetrable for liquid present the electrodes. Anodes, located at $\pm d_a$, are maintained at the constant positive potential φ_a : $q\varphi_a/kT \gg 1$ relative to the potential of the cathodes, located at $\pm d_c$. The upper portion of the Figure 2 presents the configuration of the planar signal converting cell and illustrates the correspondence of the parameters from the equations to the real cell geometry.

Suppose that the hydrodynamic velocity is changed harmonically $V = V_0 \exp(i\omega t)$. Since practical MET sensors operate at very small hydrodynamic velocities, let's look for the solutions of equations (5) in the expansion set of powers V_0 :

$$\begin{aligned} C_{I_3^-} &= C_{I_3^-}^{(0)} + C_{I_3^-}^{(1)} \\ \Phi &= \Phi^{(0)} + \Phi^{(1)} \end{aligned} \tag{17}$$

Here, $C_{I_3^-}^{(0)}, \Phi^{(0)} \sim V^0$ $C_{I_3^-}^{(1)}, \Phi^{(1)} \sim V^1$.

Substituting into **Error! Reference source not found.** and taking into consideration that $q\varphi_a/kT \gg 1$ and $q\Phi^{(1)}/kT \ll 1$, gives:

$$\begin{aligned} C_{I_3^-,anode}^{(0)} &= C_a; \\ C_{I_3^-,cathode}^{(0)} &= 0; \\ C_{I_3^-,s}^{(1)} &= -2C_{I_3^-,s}^{(0)} q\Phi^{(1)}/kT \end{aligned} \tag{18}$$

C_a is the concentration of I_3^- distant from the electrodes. Note that variable concentration on the cathode $C_{I_3^-}^{(1)}$ is always 0, due to the second equation in (18). Variable part of the anodic concentration depends on the electrical potential and could be either positive or negative. In any case, according to the assumption of the hydrodynamic velocity smallness, the total concentration $C_{I_3^-}$ is always positive, as it must correspond to the physical meaning of this variable.

3. RESULTS AND DISCUSSION

Details of the method to solve (5) with the boundary conditions (7), (9) and (18) are given in [15]. Here are only the final results for the concentration and electrical potential distribution:

$$\left\{ \begin{array}{l} C_{I_3^-}^{(0)} = C_a, x < -d_a \\ C_{I_3^-}^{(0)} = C_a \frac{-x-d_c}{d_a-d_c}, -d_a < x < -d_c \\ C_{I_3^-}^{(0)} = 0, -d_c < x < d_c \\ C_{I_3^-}^{(0)} = C_a \frac{x-d_c}{d_a-d_c}, d_c < x < d_a \\ C_{I_3^-}^{(0)} = C_a, x > d_a \end{array} \right. \quad (19)$$

$$\frac{C_{I_3^-}^{(1)}}{C_a} = Q\lambda\omega e^{\lambda(d_a+x)}(e^{\lambda d_a} - e^{\lambda d_c}) \frac{d_a - d_c}{e^{\lambda d_a} + e^{\lambda d_c} + 2\Lambda(d_a e^{\lambda d_a} - d_c e^{\lambda d_c})}; x < -d_a$$

$$\frac{C_{I_3^-}^{(1)}}{C_a} = -Q \times$$

$$\times \left(1 - \frac{e^{\lambda(d_a+d_c+x)} + e^{-\lambda x} + \Lambda(e^{\lambda(d_c+x)}(d_a(2e^{\lambda d_a} - e^{\lambda d_c}) - d_c e^{\lambda d_c}) + e^{-\lambda x}(d_a - d_c))}{e^{\lambda d_a} + e^{\lambda d_c} + 2\Lambda(d_a e^{\lambda d_a} - d_c e^{\lambda d_c})} \right);$$

$$\frac{C_{I_3^-}^{(1)}}{C_a} = 0; -d_c < x < d_c \quad (20)$$

$$\frac{C_{I_3^-}^{(1)}}{C_a} = Q \times$$

$$\times \left(1 - \frac{e^{\lambda(d_a+d_c-x)} + e^{\lambda x} + \Lambda(e^{\lambda(d_c-x)}(d_a(2e^{\lambda d_a} - e^{\lambda d_c}) - d_c e^{\lambda d_c}) + e^{\lambda x}(d_a - d_c))}{e^{\lambda d_a} + e^{\lambda d_c} + 2\Lambda(d_a e^{\lambda d_a} - d_c e^{\lambda d_c})} \right);$$

$$\frac{C_{I_3^-}^{(1)}}{C_a} = -Q\lambda\omega e^{\lambda(d_a-x)}(e^{\lambda d_a} - e^{\lambda d_c}) \frac{d_a - d_c}{e^{\lambda d_a} + e^{\lambda d_c} + 2\Lambda(d_a e^{\lambda d_a} - d_c e^{\lambda d_c})}, x > d_a$$

$$\frac{\Phi^{(1)}q}{kT} = Q\lambda\omega(e^{\lambda d_a} - e^{\lambda d_c}) \frac{d_a + d_c + 4\Lambda d_a d_c}{e^{\lambda d_a} + e^{\lambda d_c} + 2\Lambda(d_a e^{\lambda d_a} - d_c e^{\lambda d_c})}; x < -d_a$$

$$\frac{\Phi^{(1)}q}{kT} = Q\lambda\omega(e^{\lambda d_a} - e^{\lambda d_c}) \frac{x(1 + 2\Lambda d_c) + d_c(1 + 2\Lambda d_a)}{e^{\lambda d_a} + e^{\lambda d_c} + 2\Lambda(d_a e^{\lambda d_a} - d_c e^{\lambda d_c})}; -d_a < x < -d_c$$

$$\frac{\Phi^{(1)}q}{kT} = -2Q\lambda\omega(e^{\lambda d_a} - e^{\lambda d_c}) \frac{x(1 + \Lambda(d_a + d_c))}{e^{\lambda d_a} + e^{\lambda d_c} + 2\Lambda(d_a e^{\lambda d_a} - d_c e^{\lambda d_c})}, -d_c < x < d_c \quad (21)$$

$$\frac{\Phi^{(1)}q}{kT} = -Q\lambda\omega(e^{\lambda d_a} - e^{\lambda d_c}) \frac{x(1 + 2\Lambda d_c) + d_c(1 + 2\Lambda d_a)}{e^{\lambda d_a} + e^{\lambda d_c} + 2\Lambda(d_a e^{\lambda d_a} - d_c e^{\lambda d_c})}; d_c < x < d_a$$

$$\frac{\Phi^{(1)}q}{kT} = -Q\lambda\omega(e^{\lambda d_a} - e^{\lambda d_c}) \frac{d_a + d_c + 4\Lambda d_a d_c}{e^{\lambda d_a} + e^{\lambda d_c} + 2\Lambda(d_a e^{\lambda d_a} - d_c e^{\lambda d_c})}; x > d_a$$

$$\text{Here } \lambda = \frac{1+i}{\sqrt{2}} \sqrt{\frac{\omega}{D_{I_3^-}}}; Q = \frac{V_0}{i\omega(d_a - d_c)}; w = \frac{4C_a D_{I_3^-}}{C_b(D_{I^-} + D_{K^+})}; \Lambda = \lambda w \frac{e^{\lambda d_a}}{e^{\lambda d_a} - e^{\lambda d_c}}$$

Using **Error! Reference source not found.** gives the difference between cathodic currents as follows:

$$I_{out} = I_{c1} - I_{c2} = qV_0 C_a S \sqrt{\frac{2D_{I_3^-}}{\omega}} \frac{1-i}{d_a - d_c} \frac{e^{\lambda(d_a-d_c)} - 1 + 2w\lambda d_a e^{\lambda(d_a-d_c)}}{e^{\lambda(d_a-d_c)} + 1 + 2w\lambda e^{\lambda(d_a-d_c)} \frac{d_a e^{\lambda(d_a-d_c)} - d_c}{e^{\lambda(d_a-d_c)} - 1}} \tag{22}$$

Note that although $w \sim \varepsilon$, it enters the solution in a combination with other parameters, so it cannot be considered small *a priori*.

Normalized output current $I_{norm} = I_{out} / (qV_0 C_a S)$ vs frequency behavior is shown in Figure 3 and Figure 4. Figure 3 presents amplitude characteristic at the coordinates of the cathodes $d_c = 100 \mu m$ while the anode to cathode distance varies between 1 and 100 μm .

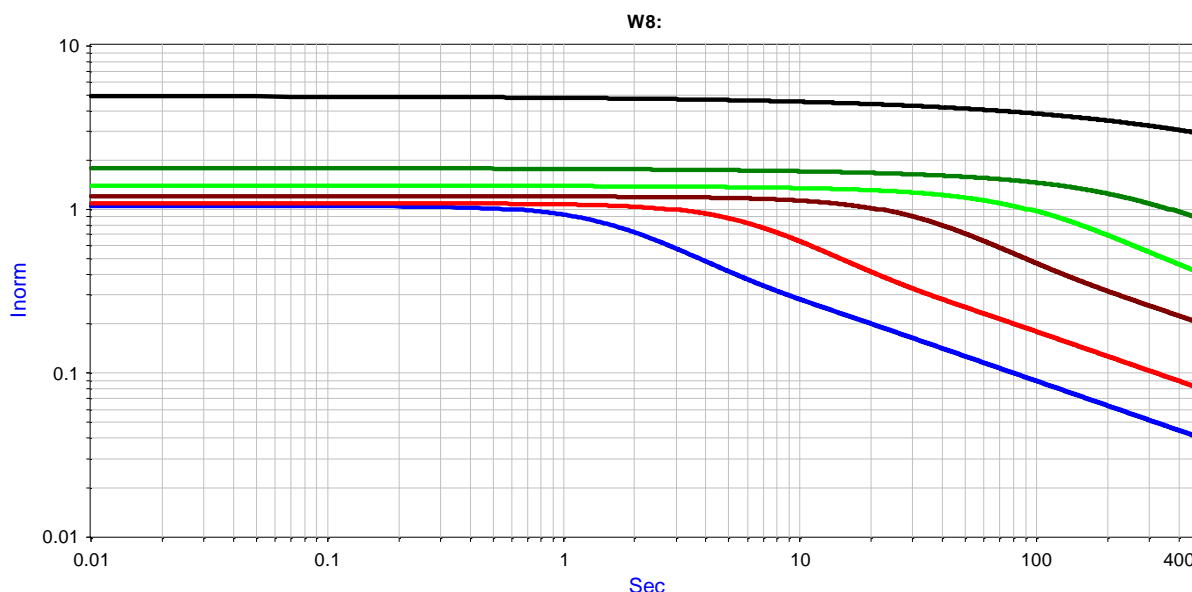


Figure 3. Amplitude vs frequency response of the signal converting cell at different distances between a cathode and the adjacent anode.

Legend:

light blue- $(d_a - d_c) = 100 \mu m$; light red - $(d_a - d_c) = 50 \mu m$; dark red - $(d_a - d_c) = 20 \mu m$; light green - $(d_a - d_c) = 10 \mu m$; dark green - $(d_a - d_c) = 5 \mu m$; black - $(d_a - d_c) = 1 \mu m$;

Other parameters used in the calculation correspond to the usual signal converting cell and are as follows: $C_a = 0.04 \text{ mol/L}$, $C_b = 4 \text{ mol/L}$, $D_{I_3^-} = 2 * 10^{-9} \text{ m}^2/\text{sec}$, $D_{I^-} = D_{K^+} = 2.4 * 10^{-9} \text{ m}^2/\text{sec}$.

Figure 4 presents amplitude vs frequency responses at a fixed distance between an anode and the adjacent cathode $(d_a - d_c) = 5 \mu m$; and the coordinates of the cathodes in the range 5 to 200 μm .

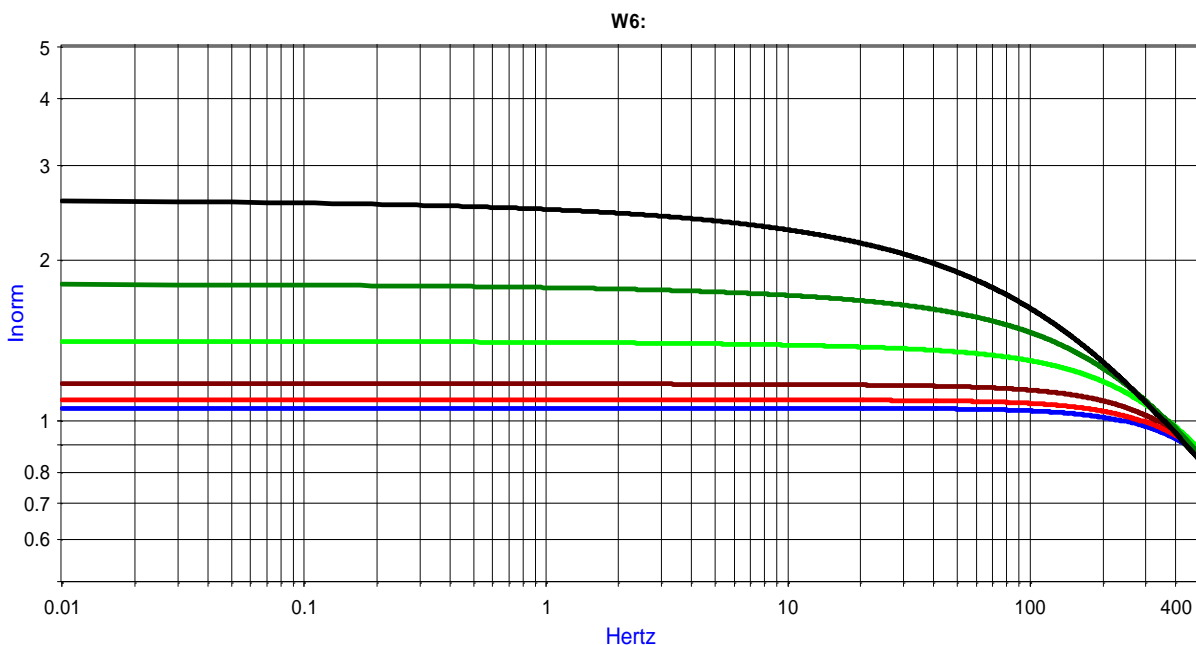


Figure 4. Amplitude vs frequency response of the signal converting cell at different coordinates of the cathodes.

Legend:

light blue- $d_c = 5\mu m$; light red - $d_c = 10\mu m$, dark red - $d_c = 20\mu m$, light green - $d_c = 50\mu m$, dark green - $d_c = 100\mu m$; black - $d_c = 200\mu m$;

It could be seen that making the distance between an anode and a cathode shorter in combination with expanding the cathode-cathode distance makes the broadband conversion efficiency higher. The sensitivity growth with the increase of the distance between the cathodes could not be explained in terms of standard convection-diffusion equation, since this approach does not take into consideration the electrical potential distribution in the electrolyte and its influence on the signal conversion factor. Moreover, one-dimensional model, based on convective diffusion equation [18] does not give any dependence on the distance between the cathodes. In two and three dimensional geometries, dependence of the sensitivity on the cathode-cathode distance could be possibly found but it has never been studied systematically [19,20,21]. The numerical studies based on the Nernst-Plank equations take into consideration the electrical potential and so they could result in the phenomenon found above, but they were limited by configurations where anode-cathode distance and cathode-cathode distance are close to each other [11,14].

Based on the presented model, the effect of the sensitivity growth could be attributed to the influence of the electrical potential as illustrated by Figure 5 and Figure 6. Here the instant distribution of concentration and electrical potential are presented. As an example, we choose time moments corresponding to the maximum (Figure 5) and the minimum hydrodynamic velocities. The red curve shows the potential instant distribution, while the blue one shows the concentration instant distribution. The green curve is given for comparison and it shows the concentration distribution in case the influence of the electrical potential is not taken into account. In this calculation, the following geometrical parameters were taken: $d_c = 100\mu m$; $(d_a - d_c) = 10\mu m$; To be specific, the signal

frequency was considered equal to 1Hz, $V_0 = \omega(d_a - d_c)$. The potential on the anodes is clear to change. In its turn, the potential change leads to the change in concentration on the anodes according to (18). In case an anode and a cathode are located close to each other, the additional diffusion flow caused by the change in concentration on the anodes reaches the cathodes and causes the current change. Figures 5 and 6 show the cathodic current change as a stronger inclination of the concentration distribution curve in the cathodic areas, which takes into account the electrical potential influence in comparison with the reference green curve.

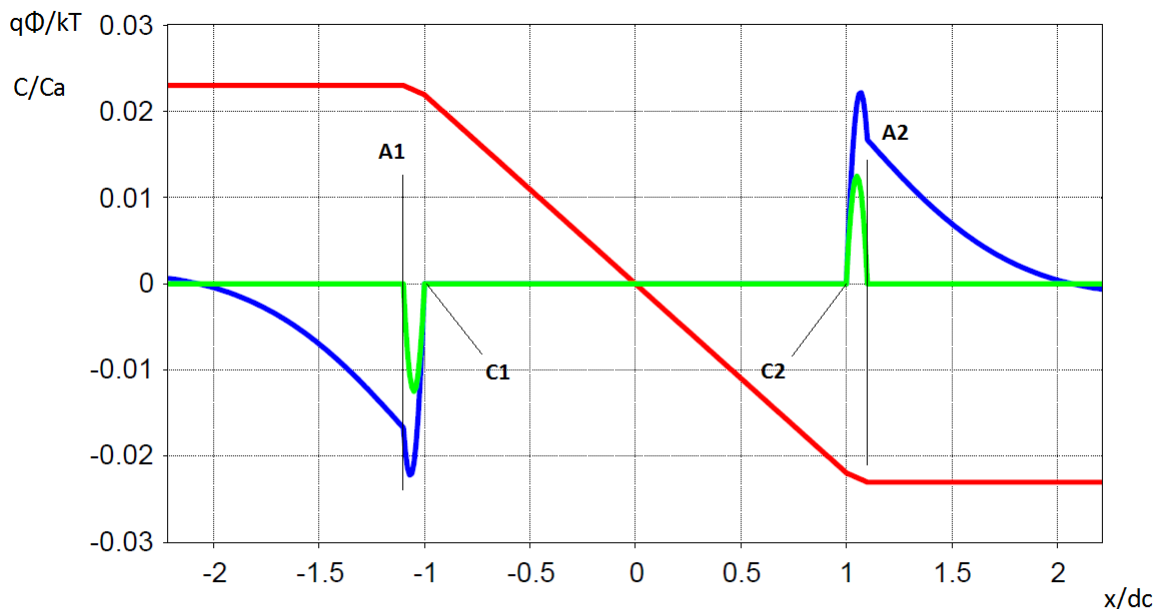


Figure 5. The distribution of non-dimensional concentration $\frac{C_{I_3}^{(1)}}{C_a}$ and the electrical potential

$\frac{\Phi^{(1)}q}{kT}$ when the oscillating hydrodynamic velocity achieves its maximum value. The signal frequency

is 1 Hz. Horizontal axis – dimensionless coordinate

Legend:

Blue curve – concentration distribution calculated according to (21).

Green curve – concentration distribution in case the influence of the electrical potential is not taken into account.

Red curve – electrical potential distribution.

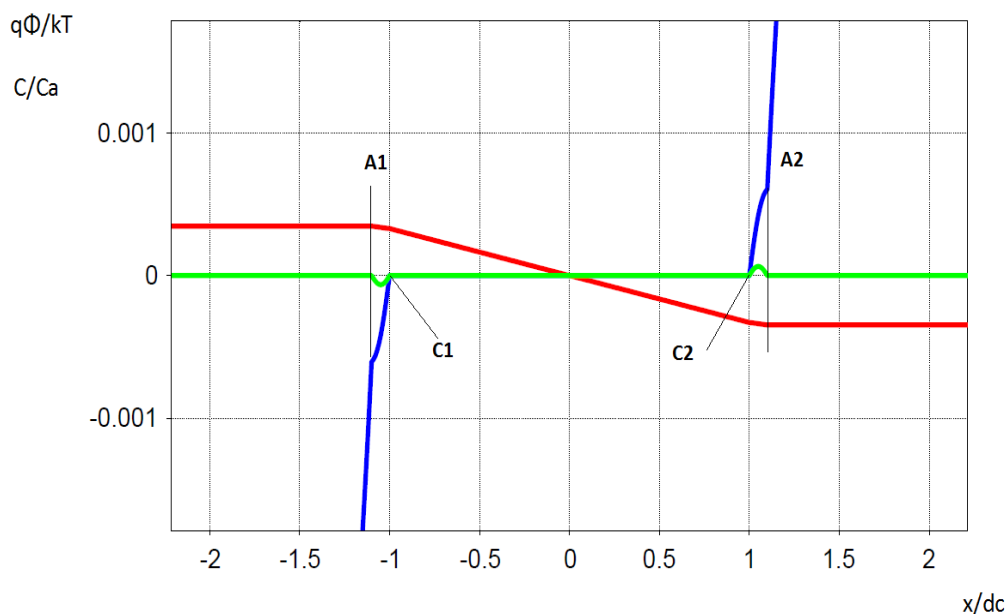


Figure 6. The distribution of non-dimensional concentration $\frac{C^{(1)}}{C_a}$ and the electrical potential $\frac{\Phi^{(1)}q}{kT}$ when the oscillating hydrodynamic velocity achieves its minimal value. The signal frequency is 1 Hz. Horizontal axis – dimensionless coordinate

Legend:

Blue curve – concentration distribution calculated according to (21).

Green curve – concentration distribution in case the influence of the electrical potential is not taken into account.

Red curve – electrical potential distribution.

Qualitatively, the effect has the following explanation. Suppose the liquid flow is directed from left to right, as it is shown in Figure 2. In this case, the left cathode receives electrolyte flow, which provides it with the additional amount of active agent. Otherwise, the right cathode receives the solution poor in active ions. In the result, the cathodic current of the left side of the cell is higher than of the right one. The condition of general electroneutrality maintenance requires the electrical current in the inter-cathode space to flow from left to right. In the result, the electrolyte potential in the left part becomes lower than in the right part. The potential change is not high, it is considerably less than the 300 mV, potential difference applied between a cathode and the adjacent anode. It has no practical influence on the cathodic currents which are defined by the speed of active component delivery. At the same time, the intensity of anodic processes stimulated by the change in electrolyte potential significantly increases on the left anode and decreases on the right one. In the result, the left anode starts producing a larger amount of electroactive ions that reach the adjacent cathode, which additionally increases the electrical current passing through it. Similarly, the decrease in speed of

anodic reactions on the right anode decreases the current through its adjacent cathode. Overall increase in output signal current is observed in comparison with the case of infinitely conductive electrolyte. The effect is larger in case of larger distance between cathodes due to the larger potential difference between the electrodes.

The above qualitative interpretation is not specific for one-dimensional system, so the discovered regularity in output current increase with the increase of inter-cathode distance relative to the distance between an anode and the adjacent cathode can be expected to be a universal result. The practical use of the predicted results is possible for the cells produced by microelectronics methods.

4. CONCLUSIONS

Analytical modelling has been done in the presented paper to study the charge transfer in four-electrode electrochemical cell which is used as a sensing element for motion sensors known as MET sensors. Similar to previously published approaches, we assume the background electrolyte (potassium iodide) to be present in high concentration, so that the electrical field beyond the double layer is weak and the migration component in the electroactive ions (tri-iodide) transportation could be neglected. Meanwhile, the dependence of electrochemical reactions at the electrodes on the electrical potential variations in the electrolyte volume adjacent to the electrodes was taken into account. In the result, the mathematical formulation of the problem includes the convection-diffusion equation for electroactive ions and Laplace type equation for electrical potential. The boundary conditions on the electrodes are presented by the equations, which bounds the concentration and the potential on the surface of electrodes. The conversion coefficient of the sensing electrochemical cell has been calculated in the frequency range between 0 and 500 Hz for one-dimensional model of electrochemical cell. The practically important result is the significant growth of the sensitivity in configurations where the inter-cathode distance is larger than the distance between a cathode and the adjacent anode.

ACKNOWLEDGEMENTS.

The results presented in this paper are obtained under the projects supported by the Russian Ministry of Education and Science—Project ID RFMEFI57814X0013

References

1. H. Huang, V. Agafonov, and H. Yu, *Sensors (Switzerland)*, 13 (2013) 4581.
2. Z. Sun and V. M. Agafonov, *Electrochim. Acta*, 55 (2010) 2036.
3. V. G. Krishtop, V. M. Agafonov, and A. S. Bugaev, *Russ. J. Electrochem.*, 48 (2012) 746.
4. V. Agafonov, A. Neeshpapa, and A. Shabalina, "Electrochemical Seismometers of Linear and Angular Motion," in *Encyclopedia of Earthquake Engineering SE - 403-1*, M. Beer, I. A. Kougoumtzoglou, E. Patelli, and I. S.-K. Au, Eds. Springer Berlin Heidelberg, 2015, pp. 944–961.
5. J. Makris, J. Papoullia, A. Tsambas, *Boll. di Geofis. Teor. ed Appl.*, 55 (2014) 561.
6. D. G. Levchenko, I. P. Kuzin, M. V. Safonov, V. N. Sychikov, I. V. Ulomov, and B. V. Kholopov, *Seism. Instruments*, 46 (2010) 250.
7. V. A. Kozlov, V. M. Agafonov, J. Bindler, and a. V. Vishnyakov, *Proc. Inst. Navig. Natl. Tech. Meet.*, 2 (2006) 650.

8. N. K. Kapustian, G. N. Antonovskaya, V. M. Agafonov, and K. A. Neumoin, "SEISMIC MONITORING OF LINEAR AND ROTATIONAL," in *6th European Worksho on theseismic behavior of Irregular and Complex Structures (6EWICS)*, 2011, no. 12–13 September, pp. 1–9.
9. Z. Sun, V. Agafonov, and E. Egorov, *J. Electroanal. Chem.*, 661 (2011) 157.
10. V. M. Volgin and A. D. Davydov, *Russ. J. Electrochem.*, 48 (2012) 565.
11. D. Chen, G. Li, J. Wang, J. Chen, W. He, Y. Fan, T. Deng, and P. Wang, *Sensors Actuators, A: Physical*, 202 (2013) 85.
12. T. Deng, D. Chen, J. Wang, J. Chen, and W. He, *Microelectromechanical Syst. J.*, 23 (2014) 92.
13. Z. Sun and V. M. Agafonov, *Sensors Actuators, B Chem.*, 146 (2010) 231.
14. Z. Sun and V. M. Agafonov, *Russ. J. Electrochem.*, 48 (2012) 835.
15. V. M. Agafonov, E. V. Egorov, and A. S. Bugaev, *Int. J. Electrochem. Sci.*, 10 (2015) In print.
16. D. A. Bograchev and A. D. Davydov, *Electrochim. Acta*, 47 (2002) 3277.
17. L. Bay, K. West, B. Winther-Jensen, and T. Jacobsen, *Sol. Energy Mater. Sol. Cells*, 90 (2006) 341.
18. C. W. Larkam, *J. Acoust. Soc. Am.*, 37 (1965) 664
19. V. A. Kozlov and D. A. Terent'ev, *Russ. J. Electrochem.*, 39 (2003) 401
20. V. A. Kozlov and D. A. Terent'ev, *Elektrokhimiya*, 38 (2002) 1104
21. V. M. Agafonov, A. A Orel., *Journal of "Nano and Microsystem Technique, MICROSYSTEM TECHNIQUE"*, 8 (6) (2008) 50

© 2016 The Authors. Published by ESG (www.electrochemsci.org). This article is an open access article distributed under the terms and conditions of the Creative Commons Attribution license (<http://creativecommons.org/licenses/by/4.0/>).